• Basic Research •

Integration of multi-omics data reveals dysregulated RNA methylation in retinal pigment epithelium drives age-related macular degeneration

Ya-Jun Gong[1], Zhi-Lin Zou[1], Kai-Rui Qiu[1], Qiang Wang[2], Xiao-Lai Zhou[1]

[1]State Key Laboratory of Ophthalmology, Zhongshan Ophthalmic Center, Sun Yat-Sen University; Guangdong Provincial Key Laboratory of Ophthalmology and Visual Science; Guangdong Basic Research Center of Excellence for Major Blinding Eye Diseases Prevention and Treatment, Guangzhou 510060, Guangdong Province, China

[2]Changde Hospital, Xiangya School of Medicine, Central South University (the First People's Hospital of Changde City), Changde 415000, Hunan Province, China

Co-first Authors: Ya-Jun Gong and Zhi-Lin Zou

Correspondence to: Xiao-Lai Zhou. Zhongshan Ophthalmic Center, Sun Yat-sen University, Guangzhou 510060, Guangdong Province, China. zhouxiaolai@gzzoc.com; Qiang Wang. Changde Hospital, Xiangya School of Medicine, Central South University (the First People's Hospital of Changde City), Changde 415000, Hunan Province, China. 962063425@qq.com

Received: 2025-04-08 Accepted: 2025-05-30

Abstract

● **AIM:** To investigate the role of RNA methylation in retinal pigment epithelial (RPE) cells in age-related macular degeneration (AMD).

● **METHODS:** RNA methylation-related gene expression profiles of AMD patient and normal control retinal pigment epithelium were evaluated by single-cell transcriptome from 34 samples (11 from normal donors and 23 from AMD patients). The causal relationship between RNA methylation dysfunction and AMD was analyzed by summary-data-based Mendelian randomization (SMR) using AMD GWAS data and multi-omics quantitative trait loci (QTL), including expression QTLs (eQTLs), protein QTLs (pQTLs), splicing QTLs (sQTLs), and m^6A-QTLs (mQTLs). Additionally, machine learning models were applied to validate the causal association between RNA methylation dysfunction and AMD using Bulk RNA sequencing data from 31 normal donors and 37 AMD patients.

● **RESULTS:** The single-cell transcriptome data analysis revealed massive dysregulation of RNA methylation-related gene expression in the RPE of AMD patients. SMR revealed causal associations between key RNA methylation regulators (*METTL3*, *NSUN6*, and *MRM1*, *etc.*) and AMD onset. Machine learning models further validated these findings and demonstrated a high accuracy of AMD risk prediction by using the above-identified RNA methylation-related genes: *METTL3*, *NSUN6*, and *MRM1*. Furthermore, *METTL3* and *NSUN6* were found to have a protective effect, while *MRM1* was associated with an increased risk of AMD.

● **CONCLUSION:** The results reveal the implication of dysregulation of RNA methylation-related gene expression in the RPE of AMD patients and further demonstrated a causal association between RNA methylation-related genes (*METTL3*, *NSUN6*, and *MRM1*) and AMD. These findings highlight the importance of RNA methylation in the pathogenesis of AMD and offer potential biomarkers and therapeutic targets for AMD management.

● **KEYWORDS:** age-related macular degeneration; retinal pigment epithelium; RNA methylation

DOI:10.18240/ijo.2025.09.03

Citation: Gong YJ, Zou ZL, Qiu KR, Wang Q, Zhou XL. Integration of multi-omics data reveals dysregulated RNA methylation in retinal pigment epithelium drives age-related macular degeneration. *Int J Ophthalmol* 2025;18(9):1626-1639

INTRODUCTION

Age-related macular degeneration (AMD) is a primary cause of permanent vision loss in older adults globally, characterized by drusen accumulation, retinal pigment epithelium (RPE) dysfunction, and degeneration of photoreceptors, predominantly in the central macula of the retina[1]. With population growth and aging, the global prevalence of AMD is projected to reach 288 million by 2040[2-3], necessitating measures to mitigate its significant burden on global healthcare systems and families. The development of AMD is influenced by multiple factors, including genetics, environmental exposures, and aging[4-5]. The severity of AMD is only 46%-71% attributable to genetic factors, while aging,

smoking, sunlight exposure, and diet significantly contribute to disease onset[6]. Genome-wide association studies (GWAS) have pinpointed several genetic loci linked to AMD, especially those involved in the regulation of the complement pathway[7-8]. However, the functional implications and subsequent effects of the identified AMD-associated genetic variants remain poorly understood due to the limitations of GWAS in resolving the complex relationships between genetic variants and complex traits or gene-environment interactions[8]. Therefore, novel strategies are urgently required to better understand the roles of additional factors in AMD pathogenesis and to uncover new therapeutic targets.

In recent years, increasing evidence has highlighted the importance of epigenetics in AMD pathogenesis, including DNA methylation, RNA methylation, and histone modifications[6,9-10]. The role of DNA methylation in AMD has been extensively studied. For example, the expression levels of plasma DNA methyltransferases (DNMT1, DNMT3A, and DNMT3B) have been proposed as potential biomarkers for AMD. In addition, a large-scale DNA methylation sequencing study of retinal tissue identified DNA methylation changes in 87 genes associated with AMD. Epigenetics also serves as a bridge between environmental factors and AMD. Common risk factors for AMD, such as aging, smoking, and exposure to sunlight, accumulate over a lifetime and may trigger epigenetic changes that influence the onset of the disease[9,11]. RNA methylation, an essential epigenetic modification, plays a key role in regulating multiple aspects of RNA biology, including RNA nuclear transport, stability, and translation efficiency[12]. So far, more than 170 RNA modifications have been discovered, and these modifications across messenger RNAs (mRNAs), ribosomal RNAs (rRNAs) and transfer RNAs (tRNAs)[13]. The regulation of RNA methylation involves a dynamic interplay among methyltransferases, demethylases, and specific binding proteins, and its dysregulation has been linked to pathological conditions such as aging, immune responses, neurodegenerative diseases, and hypoxic stress[14-15]. Although limited experimental evidence suggests that RNA methylation modifications influence the pathogenesis of AMD[16-19], systematic and unbiased genetic evidence exploring the causal relationship between RNA methylation and AMD is still lacking.

Traditional epidemiological and basic research have sought to explore causal relationships between various risk factors and AMD, but these approaches often encounter difficulties in eliminating confounding factors[7,20-21]. Mendelian randomization (MR) represents a methodological framework that utilizes genetic polymorphisms as instrumental variables to infer causality in exposure-outcome relationships[22]. By leveraging the concept of random allele allocation, MR avoids confounding (where common causes of exposure and outcome may distort their association) and reverse causation (where outcome or disease processes may affect the exposure)[23]. Using single-nucleotide polymorphisms (SNPs) derived from large-scale GWAS analyses, MR has identified numerous risk or protective factors associated with AMD, such as high-density lipoprotein cholesterol, omega-3 fatty acids, and mitochondrial function[24-26]. With the rapid advancement of high-throughput omics technologies, including transcriptomics, methylomics, proteomics, metabolomics, and lipidomics, researchers have integrated omics data with GWAS to create extensive molecular quantitative trait loci (molQTL) databases. These include quantitative trait loci (QTLs) for gene expression levels (eQTLs), protein abundance (pQTLs), splicing patterns (sQTLs), N6-methyladenosine (m^6A) methylation levels (mQTLs), and others[27]. Molecular quantitative trait loci (molQTLs) have emerged as an important tool for understanding the functional effects of genetic variants and revealing the causal mechanisms behind diseases or complex traits[28]. Building upon the MR framework, summary-data-based Mendelian randomization (SMR) was established to evaluate pleiotropic links between molecular phenotypes (including gene expression profiles, alternative splicing events, and protein abundance) and clinically relevant complex traits[29]. The integration of this approach with the the heterogeneity in dependent instruments (HEIDI) test (assessing heterogeneity in dependent instruments) allows for distinguishing true causal effects from extensive linkage disequilibrium spanning the genomic landscape[29].

Here, we performed single-cell transcriptome analysis and identified massive dysregulation of RNA methylation-related gene expression in the RPE of AMD patients. Moreover, we carried out SMR using AMD GWAS data and multi-omics QTLs (eQTLs, pQTLs, sQTLs, m6A-QTLs) and revealed causal associations between key RNA methylation regulators—*METTL3*, *NSUN6*, and *MRM1*—and AMD risk. Finally, we validated the risk prediction of the above-identified RNA methylation-related genes by utilizing machine learning. Our study revealed the implication of dysregulation of RNA methylation-related gene expression in the RPE of AMD patients and further demonstrated, for the first time, a causal relationship between RNA methylation-related genes (*METTL3*, *NSUN6*, and *MRM1*) and AMD. These findings highlight the importance of RNA methylation in the pathogenesis of AMD and offer potential biomarkers and therapeutic targets for AMD management.

MATERIALS AND METHODS

Study Design To identify genetic susceptibility features of RNA methylation-related genes, we extracted 94 RNA methylation-related genes from the Gene Ontology (GO)

database under the term "GOBP_RNA_METHYLATION" (GO:0001510). First, we analyzed the mRNA expression of RNA methylation-related genes and functional enrichment of differentially expressed genes in AMD patients using single-cell transcriptome data from human RPE/choroid tissues (GSE230348). Next, we extracted instrumental variables (IVs) for the 94 RNA methylation-related genes from eQTLs, sQTLs, pQTLs, and mQTLs. These IVs were then integrated with AMD GWAS data from the FinnGen project for SMR analysis. Finally, we validated the RNA methylation-related genes identified through SMR using machine learning models to predict AMD risk in patients.

Data Source Single-cell transcriptome data of human RPE/choroid tissues were obtained from the Gene Expression Omnibus (GSE230348). This dataset includes 34 samples (11 from normal donors and 23 from AMD patients covering early-intermediate, intermediate, and late stages of AMD). Bulk RNA sequencing data of human RPE/choroid tissues were sourced from a study by Newman *et al*[30] (GSE29801), comprising 31 samples from donors' eyes and 37 from AMD patients covering early-intermediate, intermediate, and late stages of AMD. The average age of AMD patients was 80.77±10.48y, while that of controls was 63.99±22.15y. Blood-derived eQTLs were acquired from the eQTLGen Consortium[31], which includes 10 317 trait-associated SNPs from 31 684 individuals. Genetic associations with circulating protein levels were derived from a pQTLs study conducted by Võsa *et al*[32]. The m^{6}A methylation phenotype file was obtained from Xiong *et al*[33], encompassing m^{6}A peaks from 91 donors and 4 tissues (brain, lung, muscle, and heart). We requested the sQTLs summary data from Qi *et al*[34], based on 2865 brain tissue samples. Summary-level AMD GWAS data were obtained from the FinnGen project, which includes 11 023 AMD cases and 419 198 controls[35].

Summary-data-based MR Analysis SMR analysis was performed using the SMR software (v1.3.1). For eQTLs, pQTLs, sQTLs, and m^{6}A-QTLs dataset, SMR analysis was conducted as previously described to evaluate potential causal relationships between RNA methylation-related genes and AMD[29,36]. In summary, x, y, and z represent the exposure, outcome, and instrumental variable, respectively. In MR, the effect of the exposure on the outcome (bxy) is estimated as the ratio of the instrument's effect on the outcome (bzy) to its effect on the exposure (bzx). To identify significant associations, a threshold of P_{SMR}<0.05 was applied. Multiple testing correction was performed using the false discovery rate (FDR) approach. Additionally, HEIDI test was employed to determine whether the detected SMR associations were driven by pleiotropy or linkage disequilibrium (LD). Only genes passing the HEIDI test (P_{HEIDI}>0.01) were retained for further analysis, ensuring robust causal inference. The visualization of SMR analysis results was performed using the "qqman" R package (v0.1.9).

Single-cell Transcriptome Data Analysis Single-cell RNA sequencing data from 34 RPE/choroid samples, comprising tissues from normal donors and those with AMD, were analyzed in this research. All samples underwent rigorous quality control to ensure data reliability. The Seurat package (v5.1.0) was used for processing and analyzing the single-cell data. With default parameters unless otherwise specified. First, data from 34 samples were integrated using the merge function in Seurat. Subsequently, stringent quality control was applied: cells containing less than 300 identified genes, mitochondrial gene content exceeding 15%, or UMI counts below 500 or above 30 000 were excluded. The SCTransform function was utilized to normalize data and stabilize variance, incorporating regression to adjust for the influence of mitochondrial gene expression and cell cycle variations.

Dimensionality reduction was performed through principal component analysis (PCA), with the first 50 principal components retained for subsequent cell clustering at a resolution of 0.8. Cellular subpopulations were then visualized using Uniform Manifold Approximation and Projection (UMAP). Batch effects between samples were corrected using the RunHarmony function from the Harmony package (v1.2.1).

Based on well-established marker genes, 11 major cell types were identified, including T/NK cells (*CCL5*), macrophages (*CD74*), fibroblasts (*COL1A2*), melanocytes (*MLANA*), endothelial cells (*FLT1*), retinal pigment epithelium cells (*RPE65*), pericytes (*ACTA2*), B cells (*CD79A*), Schwann cells (*PLP1*), mast cells (*FLT1*), and rod cells (*RHO*). Cell clusters that could not be confidently annotated were labeled as "Unknown" and excluded from downstream analyses.

High-dimensional weighted gene co-expression network analysis (hdWGCNA) was implemented on single-cell transcriptomic datasets to detect co-expression modules correlated with age-related macular degeneration. From the single-cell RNA-seq dataset, RPE cells were specifically extracted for weighted co-expression network analysis. After removing mitochondrial and ribosomal gene components and applying a 50-gene module size cutoff, network modules were generated. The 200 most interconnected genes per module, identified as pivotal regulatory elements, underwent GOBP functional annotation, culminating in the visualization of the ten most enriched biological pathways.

The identification of cell-type-specific transcriptional differences was conducted through Seurat's FindAllMarkers algorithm, applying stringent criteria of $|\log_2 FC|>0.5$ and adjusted P-value<0.05 for significance determination.

Significantly upregulated and downregulated genes were separately subjected to GO enrichment analysis, and the top 10 enriched GO terms were visualized.

The enrichment scores of RNA methylation-associated genes across individual cells were computed using the AUCell package (version 1.26.0)[37], employing the "area under the curve" (AUC) as the evaluation criterion.

Machine Learning Expression profiling data from 68 human eyesand their corresponding clinical information were used for machine learning. The raw microarray data generated by the Agilent-014850 Whole Human Genome Microarray (4×44K G4112F), were log-transformed for normalization.

The dataset comprising 157 sampleswas divided randomly, with 70% allocated to the training set and the remaining portion designated as the validation set. The dependent variable was the presence or absence of AMD, while independent variables included 19 genes identified through SMR analysis. Logistic regression was employed for the initial analysis, with a significance threshold of 0.05. Three significantly associated genes were selected for subsequent model construction.

To investigate associations between RNA methylation-associated gene expression patterns and AMD susceptibility, we implemented three machine learning approaches: eXtreme Gradient Boosting (XGBoost), Gradient Boosting Machine (GBM) and random Forest (RF). LASSO regression (implemented using the "glmnet" R package) was applied to rank risk and protective genes based on their importance. The models' predictive accuracy was evaluated using receiver operating characteristic (ROC) curve analysis, with performance measured by the AUC. Based on the results of LASSO regression, a nomogram was constructed to visualize the AMD risk prediction model.

RESULTS

Dysregulated RNA Methylation in RPE/Choroid Tissue of AMD Patients To investigate the role of RNA methylation in AMD, we extracted and analyzed the single-cell sequencing data of RPE/choroid tissues from AMD patients (n=23) and healthy controls (n=11; GSE230348; Figure 1A). After dimensionality reduction, the cells were divided into 12 cell types (Figure 1B-1C), with no batch effects observed between the samples. The cellular proportion results showed a significant increase of fibroblasts (P=0.034) but RPE cells in AMD patients slightly decreased (P=0.023; Figure 1D). The hdWGCNA was further performed and identified a total 21 significant modules in AMD (10 positively correlated modules and 11 negatively correlated modules; Figure 1E). The RNA methylation was identified as one of the top significant biological processes in negatively correlated module 7 by the GO functional enrichment analysis (Figure 1F). Consistently, the transcriptional levels of RNA methylation-related genes were also reduced in the RPE/choroid tissues of AMD patients (Figure 1G). Together, these data suggest that changed RNA methylation level is associated with AMD and its dysregulation may contribute to AMD pathogenesis.

Dysregulated RNA Methylation in RPE of AMD Patients Given that the pathogenesis of AMD is closely related to RPE cells, we further explored the RNA methylation-related genes in RPE cells. The volcano plot showed that there were a total of 1335 DEGs (483 downregulated, 852 upregulated) in RPE cells (Figure 2A). The GO functional enrichment analysis of DEGs revealed that RNA metabolism and processing were among the top downregulated biological processes in RPE cells of AMD patients (Figure 2B). RNA metabolism and processing were known to be tightly regulated by RNA methylation[12]. Moreover, RNA methylation-related genes were significantly downregulated in RPE cells (Figure 2C).

To further explore the relationship between RPE cell heterogeneity and AMD, we performed unsupervised dimensionality reduction clustering of RPE cells, and ultimately divided RPE cells into three clusters (Figure 2D). In cluster 1, the expression levels of RNA methylation-related genes were the lowest, while clusters 0 and 2 had higher expression levels of these genes (Figure 2E). Interestingly, the proportion of RNA methylation in lower cluster 1 RPE cells was the highest among the three clusters in AMD patients, while the proportion of RNA methylation in higher clusters 0 and 2 RPE cells was enriched in healthy controls (Figure 2F). To explore the function of these three clusters of RPE cells, we extracted their hub genes (Figure 2G) and performed GO enrichment analysis of the hub genes (Figure 2H-2J). As the GO enrichment analysis showed the hub genes enriched in cluster 0 were predominantly associated with processes involved in maintaining cellular homeostasis, such as chaperone-mediated autophagy (*EEF1A1* and *HSP90AA1*) (Figure 2H, 2K). The hub genes enriched in cluster 2 were principally related to maintaining normal vision, such as visual perception (*RDH5* and *RLBP1*; Figure 2J, 2M). In contrast, the hub genes enriched in cluster 1 were primarily linked to RNA metabolism, such as regulation of miRNA catabolic process (*MALAT1* and *NEAT1*; Figure 2I, 2L). These results indicated that cluster 0 and 2 RPEs are likely normal functional or protective RPEs, while cluster 1 RPE cells may represent the disease-associated RPE cells in AMD.

Based on the RNA methylation-related gene expression profiles and the results of GO enrichment analysis, we combined clusters 0 and 2 into a group called high-methylation RPE cells, and cluster 1 was named low-methylation RPE cells (Figure 3A-3B). We then performed hdWGCNA analysis on these two groups of cells (Figure 3C). The hdWGCNA analysis revealed a total of 15 different modules: 9 negatively

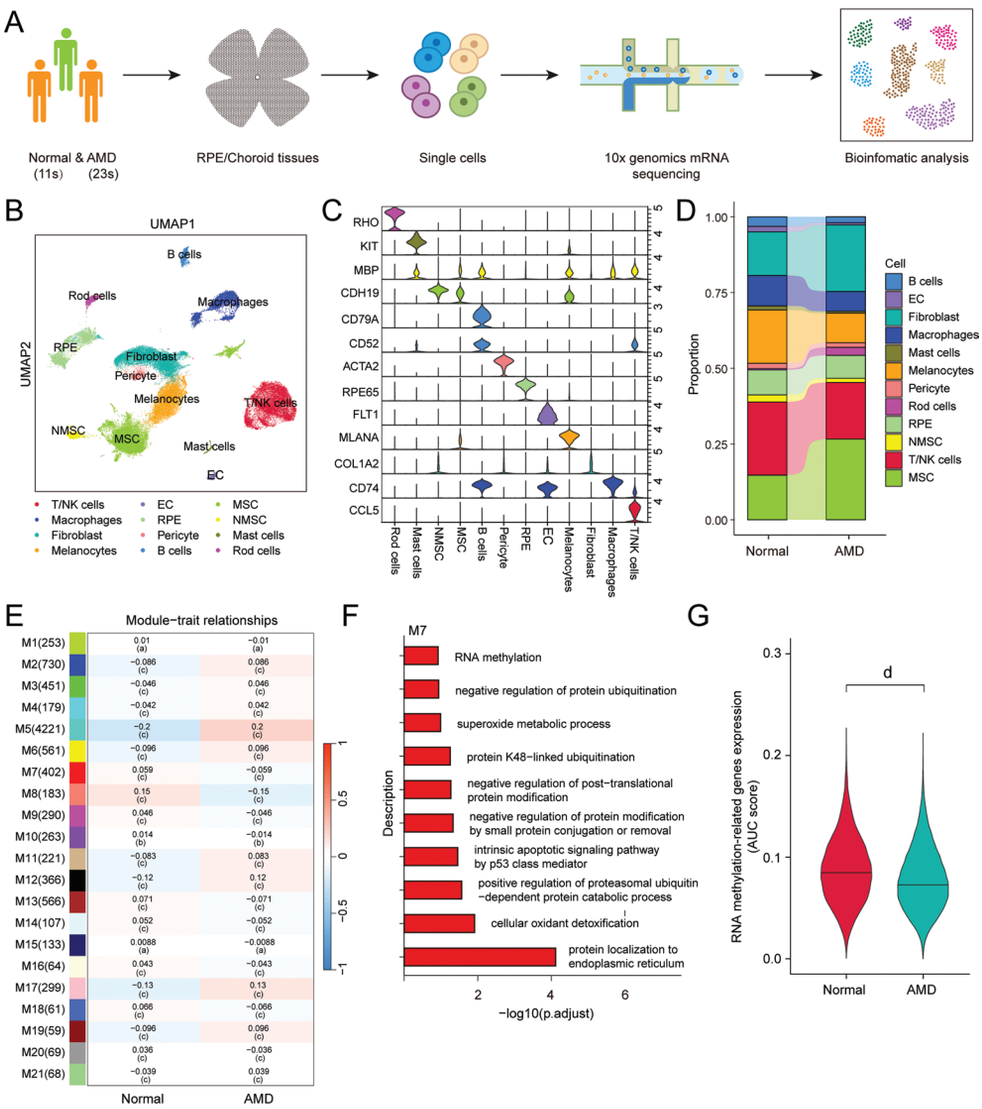

Figure 1 Dysregulated RNA methylation in RPE/choroid tissue of AMD patients A: Schematic diagram of sample processing and experimental flow of single-cell transcriptome. B: The UMAP plot was used to visualize the 11 identified RPE and choroidal clusters. Cell clusters that could not be confidently annotated were labeled as "Unknown" and excluded from downstream analyses. C: The violin plots of marker genes of distinct cell types. D: Proportion of all types of cells in AMD and control group. E: Module-trait relationships were plotted for normal controls and AMD patients. These plots were generated with hdWGCNA for groups of genes that increase (red) or decrease (blue) together. A unique color was assigned to each of these groups (modules). Correlations and *P*-values were shown for the different populations (AMDs *vs* controls). F: GO enrichment analysis of the M7 module showed the top 10 biological processes. G: The violin plot displays the mRNA expression levels of RNA methylation-related genes across all cells in the AMD and normal groups, with expression levels calculated using the AUCell R package. [a]*P*<0.05; [b]*P*<0.01; [c]*P*<0.001; [d]*P*<0.0001. EC: Endothelial cell; RPE: Retinal pigment epithelium; AMD: Age-related macular degeneration; UMAP: Uniform Manifold Approximation and Projection; hdWGCNA: High-dimensional weighted gene co-expression network analysis.

correlated ones and 6 positively correlated ones (Figure 3D). The GO analysis of negatively correlated modules further showed the suppression of multiple biological processes of energy production (Figure 3E), material metabolism (Figure 3F), and RNA metabolism (Figure 3G) in low-methylation RPE cells. Notably, the inhibition of these biological processes was linked to the pathogenesis of AMD[38-40]. These data reveal that the dysregulated RNA methylation in RPE cells may lead to RPE dysfunction, which ultimately contributes to the development of AMD.

Potential Causal Role Between RNA Methylation Dysfunction and AMD To evaluate the potential causal association between RNA methylation and AMD, we performed SMR analysis using eQTLs of 65 SNPs of RNA methylation-related genes and AMD GWAS data. This analysis identified 6 associated SNPs (Figure 4A), and these SNPs passed the HEIDI test, indicating that these SNPs are strong association signals and not due to pleiotropy. Among these 6 SNPs correlated genes, *METTL3* (rs61973223), *MRM3* (rs2273454), *GTPBP3* (rs117419016), and *TRDMT1*

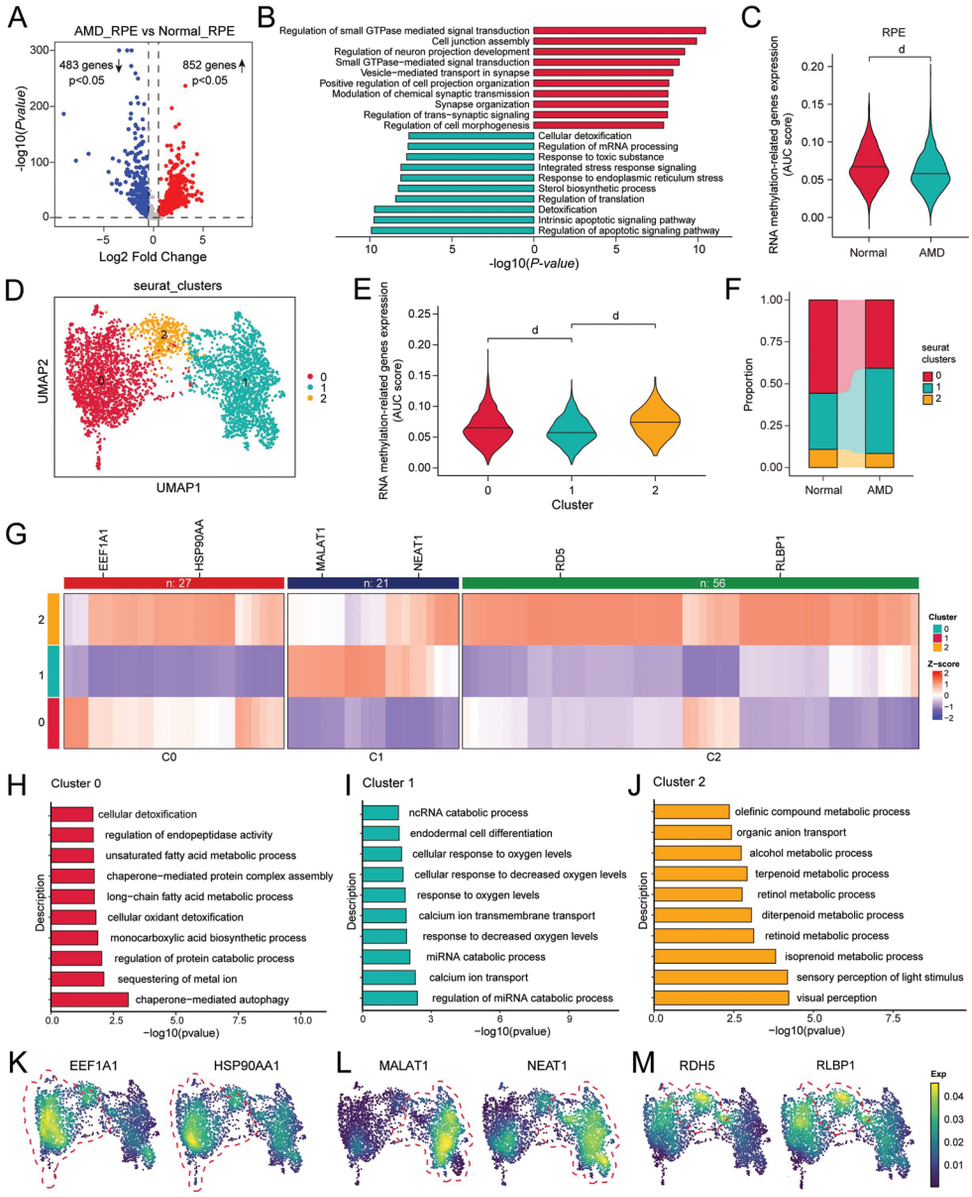

Figure 2 Dysregulated RNA methylation in RPE of AMD patients A: The volcano plot shows the DEGs in the RPE cells of AMD patients and normal controls. Genes with $|\log_2 FC|>0.5$ and $P<0.05$ were considered significantly differentially expressed. B: Top 10 GO terms enriched in upregulated and downregulated DEGs. The red and green bars indicate upregulated and downregulated terms. C: The violin plot illustrates the mRNA expression levels of RNA methylation-related genes in all RPE cells from the AMD and normal groups, with expression levels represented by the AUC score. D: The UMAP plot displays that all RPE cells from AMD and normal samples can be divided into three clusters. E: Evaluation of RNA methylation-related gene expression in the three RPE clusters. F: The bar chart shows the proportion of the three RPE cell types in the AMD and normal groups. G: Heatmap showing the hub genes of each RPE cell cluster. H-J: GO enrichment analysis was performed on the top hub genes of each RPE cell cluster in G. K-M: The average expression of representative DEGs was projected on the UMAP plot. *EEF1A1* and *HSP90AA1* were representative hub genes of cluster 0 (K), *MALAT1* and *NEAT1* were representative hub genes of cluster 1 (L), and *RDH5* and *RLBP1* were representative hub genes of cluster 2 (M). $^{d}P<0.0001$. DEG: Differentially expressed genes; RPE: Retinal pigment epithelium; AMD: Age-related macular degeneration; UMAP: Uniform Manifold Approximation and Projection.

(rs2356829) were negatively correlated with disease onset, with *METTL3* (rs61973223) showing the strongest negative correlation [odds ratio (OR): 0.83, 95% confidence interval (CI): 0.76-0.92], while *FTSJ3* (rs2727288) and *FBL* (rs11881344) were positively correlated with disease onset, with *FBL* (rs11881344) showing the strongest positive correlation (OR: 1.18, 95%CI: 1.00-1.39; Table 1).

Similarly, we conducted SMR analysis of the sQTLs of RNA methylation-related genes with AMD GWAS data. After HEIDI test, we identified a total of 6 SNPs among the 61 SNPs of RNA methylation-related genes that met the threshold for marginal significance ($P<0.05$; Figure 4B). Among these 6 SNPs correlated genes, *FTSJ3* (rs17631783), *SNRPD1* (rs13381941), and *THADA* (rs2374551) were negatively

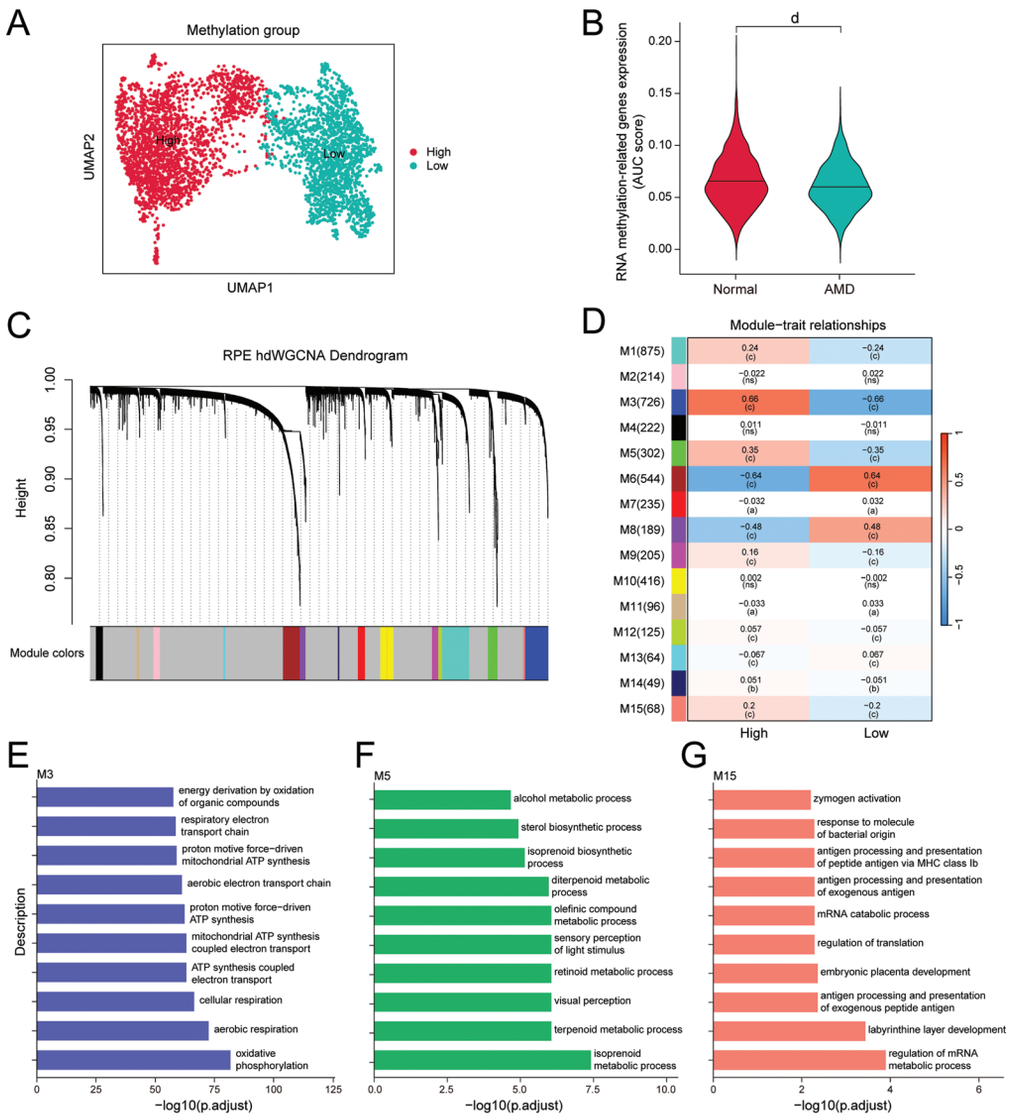

Figure 3 Dysregulated RNA methylation in RPE cells from AMD patients A: Based on the expression of RNA methylation-related genes in RPE cells, cluster 0 and cluster 2 were combined into a high methylation cluster, while cluster 1 was termed the low methylation cluster. B: Evaluation of RNA methylation-related gene expression in the high and low methylation clusters. C: Clustering dendrogram was utilized to visualize all modules in the scale-free network. Fifteen co-expression modules were constructed and were shown in different colors. D: Module-trait relationships were plotted for normal controls and AMD patients. These plots were generated with hdWGCNA for groups of genes that increase (red) or decrease (blue) together. A unique color was assigned to each of these groups (modules). Correlations and *P*-values were shown for the different populations (AMDs *vs* controls), ns: No significance. E: GO enrichment analysis of module 3 (M3) showed the top 10 enriched biological processes. F: GO enrichment analysis of module 5 (M5) showed the top 10 enriched biological processes. G: GO enrichment analysis of module 15 (M15) showed the top 10 enriched biological processes. [a]*P*<0.05; [b]*P*<0.01; [c]*P*<0.001; [d]*P*<0.0001. RPE: Retinal pigment epithelium; AMD: Age-related macular degeneration; UMAP: Uniform Manifold Approximation and Projection; hdWGCNA: High-dimensional weighted gene co-expression network analysis.

correlated with disease onset, with *SNRPD1* (rs13381941)showing the strongest negative correlation (OR: 0.61, 95%CI: 0.38-0.96), while *METTL3* (rs2242526), *TARBP1* (rs60079444), and *TRDMT1* (rs11254406) were positively correlated with disease onset, with *METTL3* (rs2242526) showing the strongest positive correlation (OR: 1.44, 95%CI: 1.12-1.88; Table 2).

We performed SMR analysis by combining the m^{6}A-QTLs of RNA methylation-related genes with AMD GWAS data. After multiple testing corrections and HEIDI test, 17 SNPs of 14 different genes met the threshold for marginal significance (P<0.05; Figure 4C). Among these significant SNPs, 8 SNPs of 7 different genes (*MEPCE*, *TRMT10C*, *THADA*, *FBLL1*, *RNMT*, *FBL*, and *FTSJ3*) were negatively correlated with disease onset, with the SNP correlated with FBL showing the strongest negative correlation (OR: 0.81, 95%CI: 0.67-0.97), while 9 SNPs of 7 different genes (*GTPBP3*, *TRDMT1*, *THUMPD3*, *TRMT61A*, *TRMT9B*, *MRM1*, and *NSUN6*)

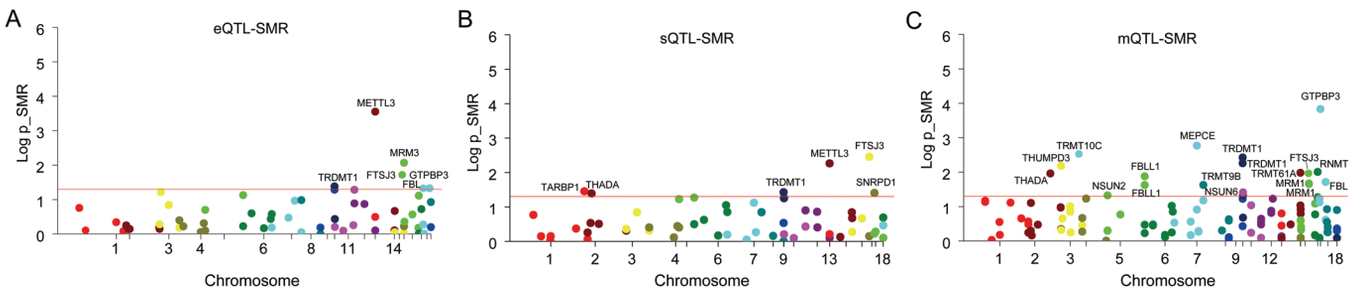

Figure 4 SMR revealed the potential causal relationship between RNA methylation in RPE cells and AMD A: Manhattan plots show the associations of eQTLs of RNA methylation-related genes with AMD GWAS data; B: Manhattan plots show the associations of sQTLs of RNA methylation-related genes with AMD GWAS data; C: Manhattan plots show the associations of m^{6}A-QTLs of RNA methylation-related genes with AMD GWAS data. SMR: Summary-data-based Mendelian randomization; RPE: Retinal pigment epithelium; AMD: Age-related macular degeneration; eQTLs: Expression quantitative trait loci; sQTLs: Splicing quantitative trait loci; m^{6}A-QTLs: m^{6}A quantitative trait loci.

Table 1 RNA methylation-related gene expression and AMD

Genes	Chr	SNP	A1	A2	P_{SMR_multi}	P_{HEIDI}	P_{FDR}	OR	OR 95%CI down	OR 95%CI up
METTL3	14	rs61973223	C	T	0.0002783	0.2948134	0.0016698	0.83	0.76	0.92
MRM3	17	rs2273454	T	G	0.0084938	0.2267236	0.0209155	0.79	0.66	0.94
FTSJ3	17	rs2727288	T	A	0.0125493	0.0997808	0.0250986	1.02	0.99	1.05
GTPBP3	19	rs117419016	A	G	0.0297439	0.2176398	0.0371800	0.99	0.92	1.08
TRDMT1	10	rs2356829	T	C	0.0412454	0.1689979	0.0494944	0.89	0.81	0.99
FBL	19	rs11881344	T	C	0.0466449	0.1005163	0.0466449	1.18	1.00	1.39

AMD: Age-related macular degeneration; SNP: Single-nucleotide polymorphism; SMR: Summary-data-based Mendelian randomization; HEIDI: Heterogeneity in dependent instruments; FDR: False discovery rate; OR: Odds ratio; CI: Confidence interval.

Table 2 RNA methylation-related gene splicing and AMD

Genes	Chr	SNP	A1	A2	P_{SMR_multi}	P_{HEIDI}	P_{FDR}	OR	OR 95%CI down	OR 95%CI up
FTSJ3	17	rs17631783	T	C	0.0034917	0.8753491	0.0209504	0.81	0.70	0.93
METTL3	14	rs2242526	C	G	0.0229307	0.0405873	0.0404891	1.44	1.12	1.88
TARBP1	1	rs60079444	T	A	0.0351359	0.0210997	0.0404891	1.08	1.01	1.16
TRDMT1	10	rs11254406	G	A	0.0374115	0.1298033	0.0404891	1.16	1.01	1.34
SNRPD1	18	rs13381941	A	G	0.0391382	0.0305095	0.0404891	0.61	0.38	0.96
THADA	2	rs2374551	G	C	0.0404891	0.1636717	0.0404891	0.93	0.86	0.99

AMD: Age-related macular degeneration; SNP: Single-nucleotide polymorphism; SMR: Summary-data-based Mendelian randomization; HEIDI: Heterogeneity in dependent instruments; FDR: False discovery rate; OR: Odds ratio; CI: Confidence interval.

were positively correlated with disease onset, with *TRMT61A* (rs117227539) showing the strongest positive correlation (OR: 1.27, 95%CI: 1.06-1.52; Table 3).

Only one SNP associated with RNA methylation-related genes was extracted from pQTLs, and no statistically significant causal relationship was identified through SMR analysis (Table 4). This result can be explained by several factors. First, RNA methylation-related proteins are typically expressed at low levels in plasma, and existing pQTL studies are predominantly based on plasma proteomics. Second, Current pQTL datasets are still underdeveloped, with only a small number of genetic variants exhibiting notable associations with protein levels being identified.

Integrating eQTLs, sQTLs, pQTLs, and mQTLs, a total of 29 SNPs of 19 RNA methylation genes associated with AMD were identified by SMR analysis. These genes may be involved in the pathogenesis of AMD through methylation modification of RNAs such as mRNAs, tRNAs, rRNAs, and small nuclear RNAs.

Machine Learning Prediction of AMD To further validate the genes identified through SMR analysis that are causally linked to AMD and their associated risk, we constructed machine learning models by combining these risk genes with bulk RNA sequencing data from the RPE/choroid of AMD patients to predict AMD (Figure 5A). After conducting logistic regression analysis, three candidate genes showed statistically significant associations: *METTL3* (OR: 0.254, 95%CI: 0.087-0.683), *NSUN6* (OR: 0.349, 95%CI: 0.136-0.823), and *MRM1* (OR: 2.461, 95%CI: 1.174-5.337; Figure 5B). We then examined the expression levels of these genes in the RPE/choroid and found that the expression of *METTL3* was significantly decreased in intermediate and advanced AMD

Table 3 RNA methylation-related gene m^{6}A methylation and AMD

Genes	Chr	SNP	A1	A2	P_{SMR_multi}	P_{HEIDI}	P_{FDR}	OR	OR 95%CI down	OR 95%CI up
GTPBP3	19	rs2364542	G	A	0.0001466	0.1539198	0.0024463	1.15	1.07	1.23
MEPCE	7	rs55721535	C	A	0.0002878	0.0740846	0.0024463	0.95	0.92	0.98
TRMT10C	3	rs4683930	T	C	0.0012072	0.0092748	0.0068414	0.87	0.80	0.95
TRDMT1	10	rs11254451	G	A	0.0037417	0.7119700	0.0159022	1.22	1.07	1.40
TRDMT1	10	rs7082679	T	G	0.0054873	0.6225775	0.0186568	1.11	1.03	1.19
THUMPD3	3	rs1145150	T	C	0.0086973	0.1411557	0.0235588	1.09	1.03	1.17
TRMT61A	14	rs117227539	A	G	0.0104107	0.7157778	0.0235588	1.27	1.06	1.52
THADA	2	rs112668841	C	G	0.0110865	0.6299417	0.0235588	0.99	0.97	1.02
FBLL1	5	rs13175257	T	C	0.0131579	0.6499245	0.0248538	0.88	0.79	0.97
RNMT	18	rs1284429	A	G	0.0183079	0.9236306	0.0297111	0.91	0.85	0.98
FBL	19	rs12982808	T	A	0.0192248	0.5380635	0.0297111	0.81	0.67	0.97
FBLL1	5	rs7446039	A	G	0.0235576	0.6137623	0.0333733	0.90	0.81	0.99
FTSJ3	17	rs2727285	A	G	0.0379083	0.4219011	0.0459045	0.95	0.89	1.01
TRMT9B	8	rs13255113	A	G	0.0417577	0.6345780	0.0459045	1.03	1.00	1.05
MRM1	17	rs4796247	C	G	0.0420322	0.7461677	0.0459045	1.07	1.01	1.13
MRM1	17	rs2411181	A	G	0.0432042	0.5454913	0.0459045	1.07	1.01	1.13
NSUN6	10	rs12767546	A	T	0.0468991	0.1024388	0.0468991	1.12	1.00	1.24

AMD: Age-related macular degeneration; SNP: Single-nucleotide polymorphism; SMR: Summary-data-based Mendelian randomization; HEIDI: Heterogeneity in dependent instruments; FDR: False discovery rate; OR: Odds ratio; CI: Confidence interval.

Table 4 RNA methylation-related protein and AMD

Gene	Chr	SNP	A1	A2	P_{SMR_multi}	P_{HEIDI}	P_{FDR}	OR	OR 95%CI down	OR 95%CI up
TRDMT1	10	rs6602180	T	C	0.594361	0.1772977	0.594361	0.94	0.89	0.99

AMD: Age-related macular degeneration; SNP: Single-nucleotide polymorphism; SMR: Summary-data-based Mendelian randomization; HEIDI: Heterogeneity in dependent instruments; FDR: False discovery rate; OR: Odds ratio; CI: Confidence interval.

patients (P=0.00013), the expression of *NSUN6* started to decrease from subclinical stage of AMD (P=0.0036), while the expression of *MRM1* was significantly elevated in intermediate and advanced AMD patients (P=0.038; Figure 5C-5E). These data suggest that the expression levels of *METTL3* and *NSUN6* are negatively correlated with the disease onset, while the expression of MRM1 is positively correlated with the disease onset. To further validate the correlation of these three identified genes with the disease onset, we performed machine learning on their expression profiling data from 68 human eyesand their corresponding clinical information to test their predictive power. To achieve this, three commonly used machine learning models: RF, XGBoost, and GBM were employed. After several rounds of training and testing, all three models showed good specificity and sensitivity, with RF performing the best (AUC=0.900), followed by XGBoost (AUC=0.839), and GBM showing relatively lower performance but still achieving an AUC of 0.785 (Figure 5F-5H). These results indicate a strong association between the expression levels of *METTL3*, *NSUN6*, and *MRM1* and the risk of developing AMD.

Since AMD patients are classified into subclinical, early, intermediate, and advanced AMD, we further evaluated the association of the above-identified three genes with disease severity by using LASSO regression (Figure 6A). LASSO regression model ranked the risk and protective genes based on their contribution and found that *METTL3* and *MRM1* had the greatest predictive power, followed by *NSUN6* (Figure 6B). The negative coefficient score of *METTL3* (-0.4) and *NSUN6* (-0.26) indicated both of these two genes were likely to function as a protective factor for AMD, while the positive coefficient score of *MRM1* (0.35) suggested its risk role in AMD (Figure 6B). Furthermore, the combination of these three genes could also achieve relatively good predictive performance for the disease severity association, with an AUC of 0.759 (Figure 6C). To enhance the accuracy of the model, we integrated the risk score with clinical factors such as age and sex to construct a nomogram, which visually represents the risk of AMD severity in patients (Figure 6D). This comprehensive approach allows for personalized risk assessment and may aid in the clinical management of AMD.

DISCUSSION

In this study, we investigated the role of RPE RNA methylation in the pathogenesis of AMD by integrating single-cell

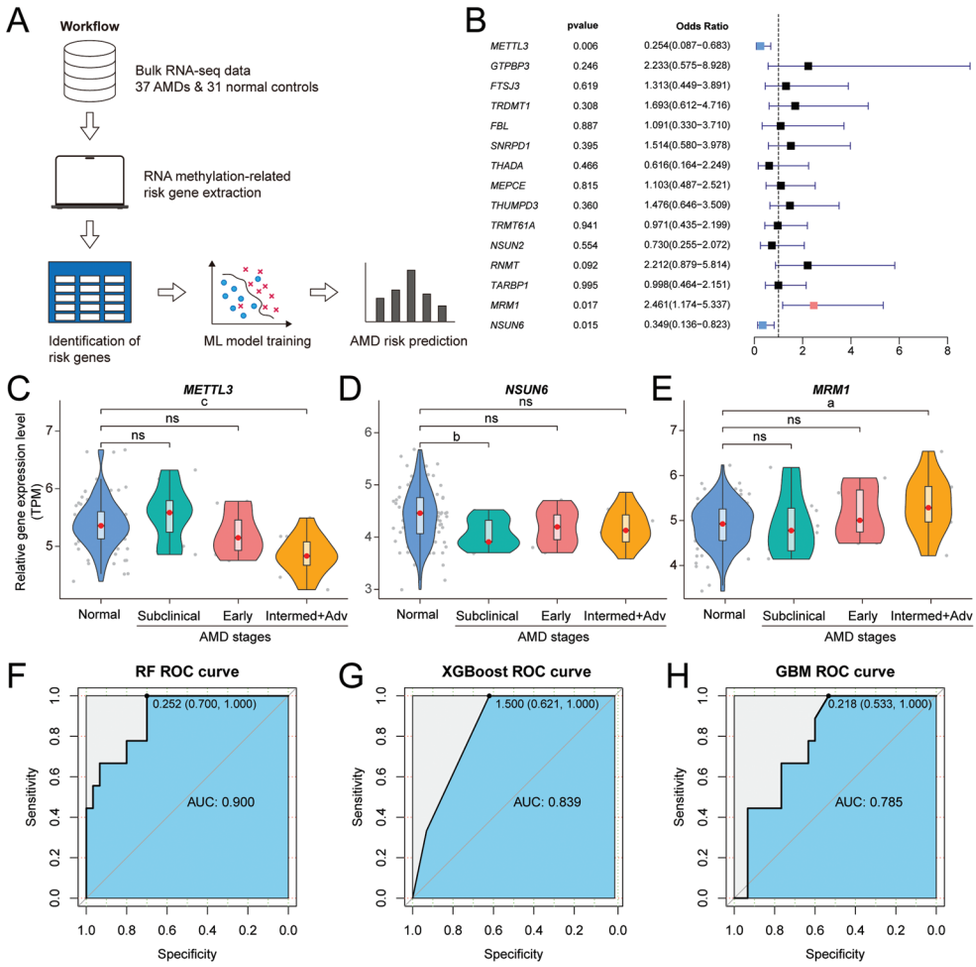

Figure 5 Machine learning prediction of AMD A: Schematic diagram of the machine learning process for identifying AMD-related genes. B: Top AMD-related candidate genes identified using logistic regression. C-E: Relative mRNA expression levels of the 3 top AMD-associated genes identified in B. [a]*P*<0.05, [b]*P*<0.01, [c]*P*<0.001. F-H: Evaluation of AMD prediction efficiency using machine learning based on identified top AMD-related genes. AMD: Age-related macular degeneration; RF: Random forest; GBM: Gradient boosting machine; XGBoost: Extreme gradient boosting; ROC: Receiver operating characteristic; AUC: Area under the receiver operating characteristic curve; TPM: Transcripts per million.

transcriptome data, SMR, and machine-learning approaches. The single-cell transcriptome data analysis revealed massive dysregulation of RNA methylation-related gene expression in the RPE of AMD patients. Furthermore, we established a causal association between RNA methylation-related genes and the onset of AMD using SMR analysis. Finally, we demonstrated the potential of RNA methylation-related genes as biomarkers for predicting AMD risk and severity using machine learning. These results provide novel insights into the epigenetic mechanisms underlying AMD and highlight the therapeutic potential of targeting RNA methylation pathways.

RNA methylation, a key epigenetic modification, is essential for numerous physiological and pathological processes, including development, aging, oxidative stress, and neurodegeneration. Interestingly, recent research has revealed its involvement in the pathogenesis of AMD as well[40-41]. Previous studies have suggested that lncRNA IPW, circSPECC, HMGA2, and ALKBH5 participate in maintaining the homeostasis of RPE cells and oxidative stress *via* RNA m^6A modification[16-19]. Our single-cell data analysis revealed a significant dysfunction of RNA methylation and associated biological processes, such as RNA metabolism, splicing, and methylation, in the RPE cells of AMD patients. This finding together with previous research indicates that epigenetic disturbances at the RNA level contribute to RPE dysfunction in AMD. RNA methylation, especially modifications such as m^6A and m^5C, is crucial for maintaining RPE homeostasis by regulating mRNA stability, stress granule formation, and protein synthesis[12-13]. The observed dysregulations in RNA methylation in AMD RPE cells may impair these protective mechanisms, leading to accumulated oxidative damage and photoreceptor degeneration.

Both coding and non-coding RNAs were subject to RNA modifications. Coding RNAs primarily include mRNA, while non-coding RNAs consist of rRNA, tRNA, and long non-coding RNA (lncRNA)[13]. Methylation of coding RNAs regulates gene expression by modulating mRNA stability and degradation, whereas methylation of non-coding RNAs

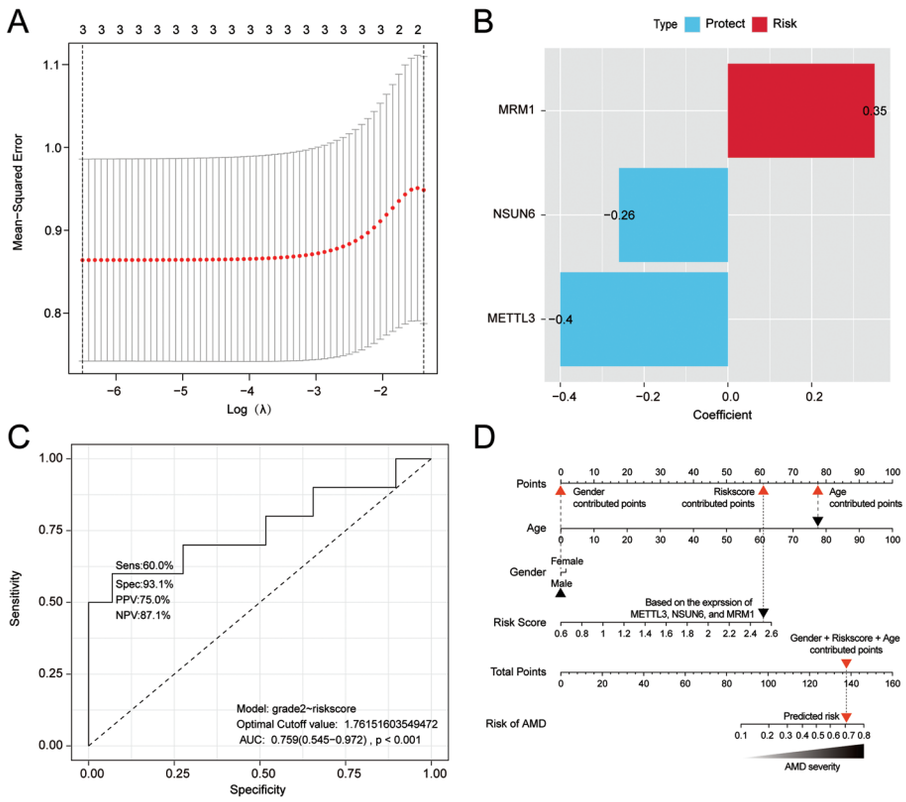

Figure 6 Machine learning for the prediction of AMD risk A: The process of feature selection. LASSO regression was applied to rank risk and protective genes based on their contribution. B: Contribution of the three most relevant genes to the AMD prediction. C: Performance for models based on the AUC of the ROC curve. D: Nomogram to predict the probability of AMD. The influence of each predictor (risk score, age, and gender) was visualized by points on the respective horizontal line and the total points correlated with the predicted risk of AMD were the sum points of the gene expressed-based risk score, age, and gender contributed points. For example, a 78-year-old male patient with advanced-stage AMD (clinically diagnosed) can be accurately predicted based on the risk score (achieved from the expression of *METTL3*, *NSUN6*, and *MRM1*), and score from age and gender by using the prediction model in C. AMD: Age-related macular degeneration; AUC: Area under the receiver operating characteristic curve; ROC: Receiver operating characteristic.

shapes their structure and adjusts their functions[42]. Our comprehensive SMR analysis, which included genes related to RNA methylation, identified not only the well-known m^{6}A methylation gene *METTL3*, but also methylation genes associated with rRNA and tRNA, such as *FTO*, *NSUN6*, *MRM1*, and *TRDMT1* (Figure 4). The relationship between rRNA and tRNA methylation and AMD is rarely reported, therefore our findings broaden the scope of RNA methylation's involvement in AMD.

Our SMR analysis and machine learning models identified *METTL3* as a powerful protective factor against AMD (OR: 0.254). METTL3 serves as the central catalytic subunit of the N6-methyladenosine methyltransferase complex, mediating m^{6}A site-specific deposition on mRNA, thereby influencing its stability and translation efficiency[15,43]. N6-methyladenosine modification mediated by METTL3 is one of the most common RNA modifications[44]. METTL3 maintains intracellular oxidative stress balance by regulating pathways such as TUG1/Clusterin and MAPK/JNK[45-48]. Importantly, by methylating NR2F1, METTL3 reduces inflammation in RPE cells[49]. The reduction of METTL3 in the RPE cells of AMD patients may disrupt this balance and impair the RPE's ability to resist oxidative damage. METTL3 deficiency reduces m^{6}A-dependent methylation of the Kinetochore Complex Component (MIS12), accelerating the senescence of mesenchymal stem cells. Furthermore, METTL3 levels significantly decrease during aging in tissues such as the heart and skeletal muscle of primates, highlighting its essential role in maintaining cell activity, function, and resistance to aging[50-51]. Since oxidative stress, inflammation, and aging are core mechanisms in AMD pathogenesis, the decrease of METTL3 in RPE cells may contribute to AMD development, thus m^{6}A regulation by METTL3 holds therapeutic potential.

NOP2/Sun RNA Methyltransferase 6 (NSUN6) belongs to the Nol1/Nop2/SUN domain protein family and catalyzes the m^{5}C methylation of cytosine in tRNA[52-53]. Post-transcriptional modifications of tRNA occur during several stages of its biogenesis and help maintain its specific spatial structure and thermal stability, playing a role in protein translation[54-55]. tRNA has over 90 modifications, the majority of which are

methylations or derivatives of methylated residues, with m^5C being one of the well-characterized modifications[56-57]. The human genome encodes seven putative m^5C RNA methyltransferases from the NSUN family, which contain the characteristic SUN domain. Currently, NSUN2 and NSUN6 are the primary "writers" catalyzing m^5C methylation in tRNA[58-59]. NSUN6 regulates macrophage polarization and oxidative stress through m^5C modifications[60-61]. In a clinical study encompassing 107 samples, *NSUN6* expression was found to be significantly reduced in common neurodegenerative diseases[62], and a reduction in NSUN6 methyltransferase activity causes neurological abnormalities in both humans and fruit flies[63]. Our study shows a decrease in *NSUN6* expression in early-stage AMD (Figure 5C), with a declining trend in later stages, and *NSUN6* is associated with reduced AMD risk (OR: 0.349). Therefore, we hypothesize that the reduction of *NSUN6* in RPE cells of early-stage AMD patients may lead to abnormal macrophage activation, resulting in chronic inflammation and ultimately exacerbating AMD progression.

Compared to *METTL3* and *NSUN6*, *MRM1* was upregulated in clinically diagnosed AMD and was positively associated with disease severity (OR: 2.461). MRM1 is a mitochondrial rRNA methyltransferase responsible for the site-specific formation of 2'-O-methylguanosine on mitochondrial ribosomal 16S rRNA, 21S rRNA, and 23S rRNA[64]. Research on the functional role of MRM1 is limited, but it is expected to participate in mitochondrial protein translation and control mitochondrial biogenesis, thereby maintaining mitochondrial homeostasis[65]. Studies have confirmed that MRM1 acts as an inhibitor of endoplasmic reticulum stress-induced cell death by blocking the accumulation of reactive oxygen species, promoting cell survival[66]. However, overexpression of *MRM1* can cause mitochondrial dysfunction and structural damage, ultimately leading to mitochondrial apoptosis[67]. Therefore, MRM1 may play a role in AMD pathogenesis by regulating mitochondrial function.

The main strengths of this study lie in several aspects. First, we conducted a systematic and unbiased SMR analysis analysis to explore the causal links between RNA methylation and AMD. We included all known RNA methylation-related genes (including tRNA, rRNA, circRNA, lncRNA, *etc.*), which helped eliminate selection bias. Second, our MR analysis utilized multiple datasets, including eQTLs, sQTLs, pQTLs, and m^6A-QTLs, enabling a comprehensive investigation of the causal links between RNA methylation and AMD. Third, we integrated single-cell transcriptome data, and bulk transcriptome data, and further validated the results from SMR in machine learning models, making our findings more robust.

However, there are certain limitations to this study. First, RNA methylation is a dynamic process, whereas our QTLs data represents a cross-sectional result. Therefore, future longitudinal studies tracking RNA methylation dynamics in AMD cohorts will clarify its prognostic value. Additionally, due to the limited sample size, we did not perform stratified analyses across different AMD stages. Future studies with larger cohorts will be necessary to conduct stage-specific analyses to determine the precise relationship between RNA methylation and AMD progression. Second, the absence of comprehensive RPE-specific datasets restricts our capacity to perform this validation. Given their larger sample sizes, we initially used blood-based markers for identification. However, further validation requires tissue-specific data, especially from the RPE. Finally, although our SMR analysis strongly associates RNA methylation genes with AMD, some of the genes we identified have limited research on their role in the disease. Further experimental investigations are required to validate their participation.

In this study, we investigated the potential causal relationship between RNA methylation dysregulation in RPE and AMD through an integrative multi-omics approach. Our findings revealed the dysregulation of three key RNA methylation genes: *METTL3*, *NSUN6*, and *MRM1* in AMD. By elucidating the roles of these RNA methylation regulators in RPE, our study lays the groundwork for developing targeted therapies for AMD by modulating RNA methylation pathways.

ACKNOWLEDGEMENTS

Authors' Contributions: Zhou XL, Gong YJ and Zou ZL conceived and designed the study. Zhou XL supervised the project. Wang Q collected data. Gong YJ and Zou ZL conducted bioinformatics analysis. Qiu KR helped with figure preparation. Gong YJ and Zou ZL drafted the manuscript and Zhou XL critically revised the manuscript. All authors read and approved the submitted version of the manuscript.

Data Available: The data used for analysis in this study were obtained from publicly available databases, and the relevant portals are provided in the Methods section.

Foundations: Supported by the Key Research and Development Program of the Ministry of Science and Technology (No.2022YFF1202901); the National Natural Science Foundation of China (No.82171404); the Natural Science Foundation of Guangdong Province of China (No.2023A1515011529); the Science and Technology Planning Project of Guangzhou City (No.2023A03J0181; No.2024A04J6481); the Fundamental Research Funds for the Central Universities (No.22yklj04); the Research Start-up Founds of Sun Yat-sen University (No.[2020]18); the Scientific Research Project of Hunan Provincial Health Commission (No. w20243051); Hunan Provincial Natural Science Foundation of China (No.2024JJ7003).

Conflicts of Interest: Gong YJ, None; **Zou ZL,** None; **Qiu KR,** None; **Wang Q,** None; **Zhou XL,** None.

REFERENCES

1 Guymer RH, Campbell TG. Age-related macular degeneration. *Lancet* 2023;401(10386):1459-1472.

2 Fleckenstein M, Keenan TDL, Guymer RH, *et al*. Age-related macular degeneration. *Nat Rev Dis Primers* 2021;7:31.

3 Chen JQ, Zhu YT, Li ZD, *et al*. Age-period-cohort analysis of the global burden of visual impairment according to major causes: an analysis of the Global Burden of Disease Study 2019. *Br J Ophthalmol* 2024;108(11):1605-1612.

4 den Hollander AI, Mullins RF, Orozco LD, *et al*. Systems genomics in age-related macular degeneration. *Exp Eye Res* 2022;225:109248.

5 Deng YH, Qiao LF, Du MY, *et al*. Age-related macular degeneration: epidemiology, genetics, pathophysiology, diagnosis, and targeted therapy. *Genes Dis* 2022;9(1):62-79.

6 Seddon JM, Reynolds R, Shah HR, *et al*. Smoking, dietary betaine, methionine, and vitamin D in monozygotic twins with discordant macular degeneration: epigenetic implications. *Ophthalmology* 2011;118(7):1386-1394.

7 Fritsche LG, Igl W, Bailey JN, *et al*. A large genome-wide association study of age-related macular degeneration highlights contributions of rare and common variants. *Nat Genet* 2016;48(2):134-143.

8 Advani J, Mehta PA, Hamel AR, *et al*. QTL mapping of human retina DNA methylation identifies 87 gene-epigenome interactions in age-related macular degeneration. *Nat Commun* 2024;15(1):1972.

9 Mohana Devi S, Mahalaxmi I, Kaavya J, *et al*. Does epigenetics have a role in age related macular degeneration and diabetic retinopathy? *Genes Dis* 2021;8(3):279-286.

10 Corso-Díaz X, Jaeger C, Chaitankar V, *et al*. Epigenetic control of gene regulation during development and disease: a view from the retina. *Prog Retin Eye Res* 2018;65:1-27.

11 Li XH, He SK, Zhao MW. An updated review of the epigenetic mechanism underlying the pathogenesis of age-related macular degeneration. *Aging Dis* 2020;11(5):1219-1234.

12 Zhou YJ, Kong Y, Fan WG, *et al*. Principles of RNA methylation and their implications for biology and medicine. *Biomedecine Pharmacother* 2020;131:110731.

13 Cappannini A, Ray A, Purta E, *et al*. MODOMICS: a database of RNA modifications and related information. 2023 update. *Nucleic Acids Res* 2024;52(D1):D239-D244.

14 Chen X, Sun YZ, Liu H, *et al*. RNA methylation and diseases: experimental results, databases, Web servers and computational models. *Brief Bioinform* 2019;20(3):896-917.

15 Shi HL, Wei JB, He C. Where, when, and how: context-dependent functions of RNA methylation writers, readers, and erasers. *Mol Cell* 2019;74(4):640-650.

16 Chen X, Wang Y, Wang JN, *et al*. m^{6}A modification of circSPECC1 suppresses RPE oxidative damage and maintains retinal homeostasis. *Cell Rep* 2022;41(7):111671.

17 Wang YW, Chen YH, Liang J, *et al*. METTL3-mediated m6A modification of HMGA2 mRNA promotes subretinal fibrosis and epithelial-mesenchymal transition. *J Mol Cell Biol* 2023;15(3):mjad005.

18 Wang Y, Zhang YR, Ding ZQ, *et al*. m6A-mediated upregulation of imprinted in prader-willi syndrome induces aberrant apical-basal polarization and oxidative damage in RPE cells. *Invest Ophthalmol Vis Sci* 2024;65(2):10.

19 Sun RX, Zhu HJ, Zhang YR, *et al*. ALKBH5 causes retinal pigment epithelium anomalies and choroidal neovascularization in age-related macular degeneration *via* the AKT/mTOR pathway. *Cell Rep* 2023;42(7):112779.

20 Saunier V, Merle BMJ, Delyfer MN, *et al*. Incidence of and risk factors associated with age-related macular degeneration: four-year follow-up from the ALIENOR study. *JAMA Ophthalmol* 2018;136(5):473-481.

21 Chakravarthy U, Wong TY, Fletcher A, *et al*. Clinical risk factors for age-related macular degeneration: a systematic review and meta-analysis. *BMC Ophthalmol* 2010;10:31.

22 Richmond RC, Davey Smith G. Mendelian randomization: concepts and scope. *Cold Spring Harb Perspect Med* 2022;12(1):a040501.

23 Sanderson E, Glymour MM, Holmes MV, *et al*. Mendelian randomization. *Nat Rev Meth Primers* 2022;2:6.

24 Burgess S, Davey Smith G. Mendelian randomization implicates high-density lipoprotein cholesterol-associated mechanisms in etiology of age-related macular degeneration. *Ophthalmology* 2017;124(8):1165-1174.

25 Xue CC, Li HT, Yu M, *et al*. Omega-3 fatty acids as protective factors for age-related macular degeneration: prospective cohort and mendelian randomization analyses. *Ophthalmology* 2025;132(5):598-609.

26 Chen JQ, Liu Z, Zhu YT, *et al*. Integrative multiomic analysis unveils the molecular nexus of mitochondrial dysfunction in the pathogenesis of age-related macular degeneration. *Exp Eye Res* 2024;249:110141.

27 Aguet F, Alasoo K, Li YI, *et al*. Molecular quantitative trait loci. *Nat Rev Meth Primers* 2023;3:4.

28 Ko BS, Lee SB, Kim TK. A brief guide to analyzing expression quantitative trait loci. *Mol Cells* 2024;47(11):100139.

29 Zhu ZH, Zhang FT, Hu H, *et al*. Integration of summary data from GWAS and eQTL studies predicts complex trait gene targets. *Nat Genet* 2016;48(5):481-487.

30 Newman AM, Gallo NB, Hancox LS, *et al*. Systems-level analysis of age-related macular degeneration reveals global biomarkers and phenotype-specific functional networks. *Genome Med* 2012;4(2):16.

31 Kurki MI, Karjalainen J, Palta P, *et al*. FinnGen provides genetic insights from a well-phenotyped isolated population. *Nature* 2023;613(7944):508-518.

32 Võsa U, Claringbould A, Westra HJ, *et al*. Large-scale cis- and trans-eQTL analyses identify thousands of genetic loci and polygenic scores that regulate blood gene expression. *Nat Genet* 2021;53(9):1300-1310.

33 Xiong XS, Hou L, Park YP, *et al*. Genetic drivers of m^{6}A methylation in human brain, lung, heart and muscle. *Nat Genet* 2021;53(8):1156-1165.

34 Qi T, Wu Y, Fang HL, *et al*. Genetic control of RNA splicing and its distinct role in complex trait variation. *Nat Genet* 2022;54(9):1355-1363.

35 Võsa U, Claringbould A, Westra HJ, *et al*. Large-scale cis- and trans-eQTL analyses identify thousands of genetic loci and polygenic scores that regulate blood gene expression. *Nat Genet* 2021;53(9):1300-1310.

36 Liufu C, Luo LX, Pang T, *et al*. Integration of multi-omics summary data reveals the role of N6-methyladenosine in neuropsychiatric disorders. *Mol Psychiatry* 2024;29(10):3141-3150.

37 Aibar S, González-Blas CB, Moerman T, *et al*. SCENIC: single-cell regulatory network inference and clustering. *Nat Methods* 2017;14(11):1083-1086.

38 Zhang M, Jiang NS, Chu Y, *et al*. Dysregulated metabolic pathways in age-related macular degeneration. *Sci Rep* 2020;10(1):2464.

39 Hansman DS, Ma YF, Thomas D, *et al*. Metabolic reprogramming of the retinal pigment epithelium by cytokines associated with age-related macular degeneration. *Biosci Rep* 2024;44(4):BSR20231904.

40 Tang JL, Zhou CD, Ye FX, *et al*. RNA methylation homeostasis in ocular diseases: all eyes on me. *Prog Retin Eye Res* 2025;105:101335.

41 Zhu XY, Zhou CD, Zhao SZ, *et al*. Role of m6A methylation in retinal diseases. *Exp Eye Res* 2023;231:109489.

42 Scheitl CPM, Ghaem Maghami M, Lenz AK, *et al*. Site-specific RNA methylation by a methyltransferase ribozyme. *Nature* 2020;587(7835):663-667.

43 Chien CS, Li JY, Chien Y, *et al*. METTL3-dependent N^6-methyladenosine RNA modification mediates the atherogenic inflammatory cascades in vascular endothelium. *Proc Natl Acad Sci U S A* 2021;118(7):e2025070118.

44 Jiang XL, Liu BY, Nie Z, *et al*. The role of m6A modification in the biological functions and diseases. *Signal Transduct Target Ther* 2021;6(1):74.

45 Tian Y, Xiao YH, Sun C, *et al*. N6-methyladenosine methyltransferase METTL3 alleviates diabetes-induced testicular damage through modulating TUG1/clusterin axis. *Diabetes Metab J* 2023;47(2):287-300.

46 Zhao TH, Sun DL, Long KY, *et al*. N^6-methyladenosine promotes aberrant redox homeostasis required for arsenic carcinogenesis by controlling the adaptation of key antioxidant enzymes. *J Hazard Mater* 2024;465:133329.

47 Gao Y, Wang M, Qin RY, *et al*. METTL3 deficiency aggravates hepatic ischemia/reperfusion injury in mice by activating the MAPK signaling pathway. *Int J Med Sci* 2024;21(6):1037-1048.

48 Li XZ, Jiang YZ, Sun X, *et al*. METTL3 is required for maintaining β-cell function. *Metabolism* 2021;116:154702.

49 Meng JY, Liu XY, Tang SY, *et al*. METTL3 inhibits inflammation of retinal pigment epithelium cells by regulating NR2F1 in an m^6A-dependent manner. *Front Immunol* 2022;13:905211.

50 Wu ZM, Shi Y, Lu MM, *et al*. METTL3 counteracts premature aging *via* m6A-dependent stabilization of MIS12 mRNA. *Nucleic Acids Res* 2020;48(19):11083-11096.

51 Wu ZM, Lu MM, Liu D, *et al*. m^6A epitranscriptomic regulation of tissue homeostasis during primate aging. *Nat Aging* 2023;3(6):705-721.

52 Haag S, Warda AS, Kretschmer J, *et al*. NSUN6 is a human RNA methyltransferase that catalyzes formation of m5C72 in specific tRNAs. *RNA* 2015;21(9):1532-1543.

53 Long T, Li J, Li H, *et al*. Sequence-specific and shape-selective RNA recognition by the human RNA 5-methylcytosine methyltransferase NSun6. *J Biol Chem* 2016;291(46):24293-24303.

54 Li J, Li H, Long T, *et al*. Archaeal NSUN6 catalyzes m5C72 modification on a wide-range of specific tRNAs. *Nucleic Acids Res* 2019;47(4):2041-2055.

55 Ruiz-Arroyo VM, Raj R, Babu K, *et al*. Structures and mechanisms of tRNA methylation by METTL1-WDR4. *Nature* 2023;613(7943):383-390.

56 Hori H. Methylated nucleosides in tRNA and tRNA methyltransferases. *Front Genet* 2014;5:144.

57 Meynier V, Hardwick SW, Catala M, *et al*. Structural basis for human mitochondrial tRNA maturation. *Nat Commun* 2024;15(1):4683.

58 Liu JH, Huang T, Zhang YS, *et al*. Sequence- and structure-selective mRNA m^5C methylation by NSUN6 in animals. *Natl Sci Rev* 2021;8(6):nwaa273.

59 Yang X, Yang Y, Sun BF, *et al*. 5-methylcytosine promotes mRNA export—NSUN2 as the methyltransferase and ALYREF as an m5C reader. *Cell Res* 2017;27(5):606-625.

60 Yan DL, Xie YS, Huang LY, *et al*. RNA m5C methylation orchestrates BLCA progression *via* macrophage reprogramming. *J Cell Mol Med* 2023;27(16):2398-2411.

61 Wang XY, Gong LJ, Wei C, *et al*. Inhibition of NSUN6 protects against intermittent hypoxia-induced oxidative stress and inflammatory response in adipose tissue through suppressing macrophage ferroptosis and M1 polarization. *Life Sci* 2025;364:123433.

62 PerezGrovas-Saltijeral A, Rajkumar AP, Knight HM. Differential expression of m^5C RNA methyltransferase genes NSUN6 and NSUN7 in Alzheimer's disease and traumatic brain injury. *Mol Neurobiol* 2023;60(4):2223-2235.

63 Mattioli F, Worpenberg L, Li CT, *et al*. Biallelic variants in NSUN6 cause an autosomal recessive neurodevelopmental disorder. *Genet Med* 2023;25(9):100900.

64 Lee KW, Bogenhagen DF. Assignment of 2'-O-methyltransferases to modification sites on the mammalian mitochondrial large subunit 16 S ribosomal RNA (rRNA). *J Biol Chem* 2014;289(36):24936-24942.

65 Rebelo-Guiomar P, Pellegrino S, Dent KC, *et al*. A late-stage assembly checkpoint of the human mitochondrial ribosome large subunit. *Nat Commun* 2022;13(1):929.

66 Hijazi I, Knupp J, Chang A. Retrograde signaling mediates an adaptive survival response to endoplasmic reticulum stress in *Saccharomyces cerevisiae*. *J Cell Sci* 2020;133(6):jcs241539.

67 Knupp J, Arvan P, Chang A. Increased mitochondrial respiration promotes survival from endoplasmic reticulum stress. *Cell Death Differ* 2019;26(3):487-501.